Journal of Hydrology: Regional Studies 36 (2021) 100851

Contents lists available at ScienceDirect

Journal of Hydrology: Regional Studies

journal homepage: www.elsevier.com/locate/ejrh

Evapotranspiration and biogeochemical regulation in a mountain peatland: insights from eddy covariance and ionic balance measurements

Meeruppage Gunawardhana [a,*], Ewen Silvester [b,c], Oliver A.H. Jones [d], Samantha Grover [a]

[a] Applied Chemistry and Environmental Science, RMIT University, GPO Box 2476, Melbourne, Victoria, 3001, Australia
[b] Department of Ecology, Environment and Evolution, La Trobe University, PO Box 821, Wodonga, Victoria, 3689, Australia
[c] Research Centre for Applied Alpine Ecology (RCAAE), La Trobe University, Australia
[d] Australian Centre for Research on Separation Science (ACROSS), School of Science, RMIT University, Bundoora West Campus, PO Box 71, Melbourne, Victoria 3083, Australia

ARTICLE INFO

Keywords:
Alpine *Sphagnum* Peatland
Eddy covariance
evapotranspiration
energy balance
ionic analysis
biogeochemical processes

ABSTRACT

Study Region: The mountainous catchments in the Australian Alps are one of the highest water-yielding regions within a generally dry continent. Peatlands are critical water-regulating components of these catchments, and their response to a changing climate will impact all downstream environments and water availability for human uses.

Study Focus: Mountain peatland ecohydrology, and in particular the role of evapotranspiration, remains incompletely understood. This study focused on evapotranspiration and biogeochemical regulation of "Alpine *Sphagnum* Bogs", with a case study at Watchbed Creek peatland. Eddy covariance was used to quantify evapotranspiration and combined with Penman-Monteith-based evapotranspiration to calculate an 'ecosystem vegetation coefficient' (K_{ESV}). Base-flow evapotranspiration and analyses of Cl^-, Na^+, Ca^{2+} and Mg^{2+} in peatland stream water were used to assess biogeochemical processes.

New Hydrological Insights for the Region: This work demonstrates that evapotranspiration is a major component of the water budget, 26% of annual precipitation. Further, we show how K_{ESV} calculated from direct measurements at one site may enable evapotranspiration to be modelled for other mountain catchments. The seasonally dependent nature of the biogeochemical regulation processes observed in this mountain peatland can be used as a reference to evaluate the condition of peatlands under similar synoptic weather conditions. In practice, this means that mountain ecosystem restoration can now be informed by a better understanding of the ecohydrology of these critical high mountain catchments.

1. Introduction

Peatlands are a type of wetland that is estimated to cover 2.84% of the earth's terrestrial surface, with a modelled total area of 4.23 million km^2 (Xu et al., 2018a). Peatlands occur where near-continuous waterlogging causes anaerobic conditions, limiting the

* Corresponding author.
E-mail address: s3734343@student.rmit.edu.au (M. Gunawardhana).

https://doi.org/10.1016/j.ejrh.2021.100851
Received 6 January 2021; Received in revised form 9 June 2021; Accepted 10 June 2021
Available online 16 June 2021
2214-5818/© 2021 The Authors. Published by Elsevier B.V. This is an open access article under the CC BY-NC-ND license (http://creativecommons.org/licenses/by-nc-nd/4.0/).

decomposition of plant material. Ongoing peatland survival and characteristics depend upon the chemical composition and seasonal periodicity of the water supply (Labadz et al., 2010, Gorham, 1957). Previous studies have shown that hydrological conditions are a fundamental determinant of the carbon budget and critical in peatland development and decay (Berger et al., 2019, Holden, 2005). Modelling suggests that hydrology, in particular evapotranspiration, influences temperature and hence biogeochemical cycling in peatlands (Weiss et al., 2006). However, peatland hydrology is still poorly understood, with a lack of long-term hydrological monitoring data and challenges in scaling up from plot to catchment scale, even in areas with extensive peatlands (Labadz et al., 2010, Swindles et al., 2019, Pemberton, 2005).

Evapotranspiration (ET) involves the exchange of water and energy between soil, land surface, and atmosphere by the processes of transpiration and evaporation (Liu et al., 2019). ET is a significant part of the water cycle in terrestrial systems, accounting for 60 – 65% of all precipitation that falls on the terrestrial surface of the earth (Liu et al., 2019, Wang and Dickinson, 2012). Accurate and long-term information on ET from direct measurements is critical to gaining a better understanding of the interactions between terrestrial ecosystems and atmosphere as well as understanding the underlying ecohydrological processes and addressing climate change questions (Brubaker and Entekhabi, 1996). However, ET is considered the most problematic term in the hydrological budget due to its heterogeneity across the landscape and the range of factors influencing ET processes (Fleischer et al., 2015).

ET can be measured by numerous methods and at various scales. Continuous estimation of ET can be achieved by six different methods, namely eddy covariance (EC), Bowen ratio, weighable lysimeters, scintillometer, surface water balance, and atmosphere water balance methods (Wang and Dickinson, 2012). EC is a commonly adopted technique to measure ecosystem-scale surface energy fluxes and ET, involving the determination of turbulent fluxes of energy and water from the covariance of their respective eddies (Wilson and Baldocchi, 2000, Lund et al., 2017). It is widely recognized that EC is the most defensible approach to measure fluxes of trace gas and energy between the biosphere and atmosphere (Baldocchi, 2014). EC calculations are premised upon ideal conditions, which comprise a flat, homogeneous land surface with no obstacles distorting the airflow across the surface of interest to the tower (Gerling et al., 2019). These ideal conditions are rarely encountered in actual ecosystems, and there are very few EC measurements in montane peatlands, where it is challenging to quantify evapotranspiration fluxes due to constraints of surface slope, limited fetch, and frequent dew formation on open-path sensors (Gerling et al., 2019). EC has been successfully used to explore meteorological and hydrological controls on the energy, water, and carbon soil-atmosphere exchanges in a great number of peatlands in the Northern Hemisphere, especially in the boreal region, some tropical peatlands and a few New Zealand peatlands (Runkle et al., 2014, Gerling et al., 2019, Kellner, 2001, Goodbrand et al., 2019, Alberto et al., 2011, Goodrich et al., 2017). Hammerle et al. (2007) assessed the validity of EC measurements in steeply sloping mountainous terrain and found that, with appropriate and rigorous quality control, EC can be used to quantify carbon, water and energy fluxes over montane grassland.

Actual evapotranspiration (ET) is influenced by both local climate and land surface conditions, including the gradient of water potential and the prevailing aerodynamic and surface resistances (Xueqin et al., 2009, Duffková, 2013). Potential evapotranspiration (ET_P) is the maximum theoretical ET of a well shaded and actively growing vegetation and assumes a continuous supply of sufficient water (Pereira et al., 1999, Pereira et al., 2015). The Food and Agricultural Organization (FAO) Penman-Monteith method is recommended as the standard method for calculating reference evapotranspiration (ET_O), which explains the evaporating power of the atmosphere at a specific location and time and does not consider the crop (vegetation) characteristics or soil factors (Allen et al., 1998). The crop coefficient (K_C) is the ratio of ET_P and ET_O, which is used to parameterize the physiological differences between an ecosystem's plant cover in comparison to the reference vegetation (Allen et al., 1998). As recommended by the FAO, plant water consumption can be estimated based on ET_O and quantification of actual ET in most ecosystems or cropping systems (Gerling et al., 2019, Allen et al., 1998). K_C can vary with the season due to differences in aerodynamic roughness, leaf area and albedo (Pereira et al., 1999). K_C values have been reported for various crops (Marsal et al., 2013, Piccinni et al., 2009, Zhao et al., 2018) and a few naturally vegetated surfaces (Hou et al., 2010, Monteiro et al., 2016), including quantification of a modified K_C for an ombrotrophic peat bog in Germany (Gerling et al., 2019). It is valuable to determine local K_C values for more precise modelling, for example, in regional soil hydrological modelling (Gerling et al., 2019).

Peatlands are important sites of nutrient cycling and productivity (Mitsch and Gosselink, 2007). In the Australian context, alpine peatlands are located at the top of the nation's highest yielding water catchments and have long been recognised as important as nutrient 'filters' and hydraulic 'sponges' (Costin, 1957a). More recent work has shown that nutrient uptake is seasonally variable in these systems and that their role in hydraulic buffering is largely limited to short-term storage (Karis et al., 2016, Silvester, 2009). Additionally, rather than being rain-dependent, groundwater is a significant component in headwater catchment (and therefore peatland) water budgets (Western et al., 2008), that is likely critical in sustaining these ecosystems during extended low rainfall periods. The regulation of stream water composition by these peatlands is likely a critical function in the context of downstream aquatic ecosystems, maintaining a water quality environment that is within tolerance ranges of aquatic biota (Shackleton et al., 2019). Determining ET in these ecosystems is essential for quantifying chemical transformation fluxes and developing robust hydrochemical models for biogeochemical processes within these peatlands. Moreover, our understanding of the interaction between ET and peat soil saturation (i.e. water table depth) provides critical information on the seasonal variations in aerobic and anaerobic microbial processes within the peat profile (Reddy and Delaune, 2008, Hamilton, 2010).

The aims of this study were: 1) to quantify and describe the diurnal and seasonal changes in and drivers of the energy balance in a *Sphagnum*-dominated peatland in the Australian Alps using the EC technique; 2) to analyse the temporal dynamics of the ET time series at different timescales; 3) to model the Penman-Monteith reference evapotranspiration ET_O and apply the FAO crop coefficient approach to calculate a peatland-specific 'ecosystem-soil-vegetation coefficient' (K_{ESV}) using measured ET data; 4) to identify the key factors controlling evapotranspiration; and 5) combined with ionic analyses of groundwater and peatland drainage, to apply the measured ET to further understand peatland biogeochemical regulation processes and the potential uptake or production of ionic

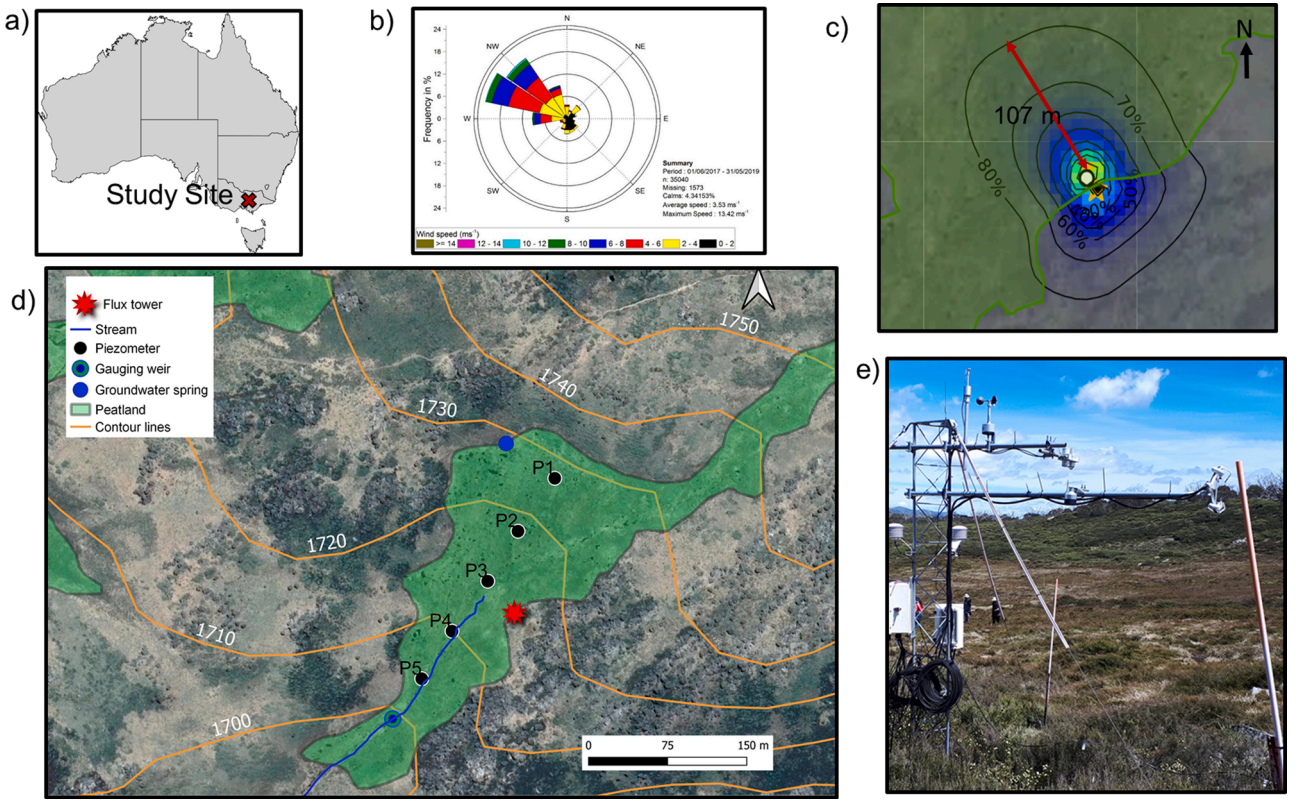

Fig. 1. a) Flux tower location in Australia; b) wind direction distribution at the tower; c) percentage coverage of peatland (green transparent overlay) within the EC source area (contours from 10 to 80% at 10% intervals); d) satellite image of the peatland showing the tower location, the main groundwater spring as well as the five piezometers (P1, P2, P3, P4, P5) and the gauging weir placement with a contour map of the of Heathy Spur-1 peatland, (map image created with Google Earth); e) eddy-covariance flux tower environment.

components that leads to regulation of stream water quality over seasonal timescales.

2. Materials and Methods

2.1. Study area

The study was conducted at a peatland (Heathy Spur-1; HS-1) in the Watchbed Creek catchment (S36° 51.882' E147° 19.0810') on the Bogong High Plains near Falls Creek in the Victorian Alpine National Park (Fig. 1). This peatland is a valley bog at an elevation of the site is 1680 – 1740 m and has been the subject of previous hydrologic and water quality studies (Silvester et al., 2021, Silvester, 2009). This region has a sub-polar oceanic climate (Cfc) with cool summers and cold, snowy winters in accordance with the Köppen Climate Classification (Beck et al., 2018). The vegetation community of the peatlands in this region is dominated by *Sphagnum* moss (*Sphagnum cristatum*) in addition to candle heath (*Richea continentis*), alpine baeckea (*Baeckea gunniana*) and rope rush (*Empodisma minus*) (Camac et al., 2017). The underlying soil is peaty organosol (Grover, 2001), with peat soils greater than 1 m deep in the lower depressions and shallower peat depths on the valley sides (less than 0.3 m). This ecosystem type is classified as an endangered ecological community (Alpine *Sphagnum* Bogs and Associated Fens ecological community) as listed by the Environmental Protection and Biodiversity Conservation (EPBC) Act 1999 (Beeton, 1999). The particular peatland studied in this work is considered to be in very good 'condition', as assessed by a range of floristic and peat soil metrics (Whinam et al., 2003) and therefore serves as a reference system for peatland rehabilitation actions.

The Heathy Spur-1 peatland is part of a relatively small headwater catchment (25.8 ha), and a particular feature of this site is the accessibility of both groundwater feed into the peatland (via one major source and several minor sources or seepages) and a gauged outflow at the peatland drainage point. The main streamline forms near the middle of the peatland, and the gauging point is located within the peatland area, with no direct terrestrial run-off (Fig. 1d). Long-term monitoring of water quality of the groundwater feed reveals that the composition of this water is essentially constant over decadal time scales (year range: 2006 – 2021; pH range: 5.25 – 5.40; electrical conductivity range: 6 – 10 μS/cm). The relatively low pH of this groundwater is largely due to CO_2 oversaturation, while the low electrical conductivity is a result of the highly weathered regolith of the Bogong High Plains (Silvester, 2009). The pH in the outflow waters varies annually over a wider range (pH range: 5.5 – 6.4), as controlled by biogeochemical processes and CO_2 evasion; electrical conductivity varies over a similar range to groundwater without a clear annual pattern (electrical conductivity range: 3.7 – 8.5). The composition of groundwater and stream water outflow is dominated by the major cations (Na^+, K^+, Ca^{2+}, Mg^{2+}) and anions (Cl^-, NO_3^-, SO_4^{2-}, HCO_3^-). Nitrate and sulphate are present at relatively low levels in the groundwater (NO_3^- range: 0 – 60 μg-N/L; SO_4^{2-} range: 55 – 100 μg-S/L) and are largely removed within the peatland through plant uptake and microbial processes (Karis et al., 2016, Silvester, 2009).

2.2. Eddy covariance systems and meteorological sensors

An eddy covariance flux tower was installed at this site in April 2017 (location: −36 ° 51' 44 S ", 147 ° 19' 15 "E; AU-APL; www.ozflux.org.au"; Fig. 1) to continuously measure fluxes of CO_2, water vapour, and energy. Fluxes analysed in this study were measured over the period from June 2017 to May 2019, which represents two complete annual cycles, starting from (southern hemisphere) winter. A combined sonic anemometer and an open-path infrared gas analyser (IRGASON, Campbell Scientific, USA) sampled the turbulent environment at 2.4 m above the land surface and frequency of 10 Hz, with the raw measurements stored in a data logger (CR3000, Campbell Scientific, USA). The tower was also equipped with a series of meteorological instruments to collect low-frequency environmental data. Air temperature (T_a) and relative humidity were measured using an HMP60 (Vaisala, Vantaa, Finland) sensor. Atmospheric pressure was measured with PTB110 sensor (Vaisala, Vantaa, Finland). Wind dynamics were measured with cup anemometer and wind vane (WAA151, Vaisala, Vantaa, Finland and W200P, Vector Instruments, UK). Incoming and outgoing shortwave and longwave radiation were measured using a CNR1 radiometer (Kipp & Zonen, Delft, Netherlands). Ancillary data were logged on the CR3000 datalogger at 30 min intervals. Two soil heat flux plates (HFP01-L, Campbell Scientific, USA) were installed at 10 cm depth in hummock and hollow micro-topographies with two averaging soil thermocouples (TCAV-L, Campbell Scientific, USA) at 2 and 6 cm below the ground.

2.3. Pre-processing, post-processing and footprint analysis

Surface turbulent fluxes of water vapour were collected at a frequency of 10 Hz, and 30 min averages were calculated via the EddyPro™ 6.2.0 open-source software (LI-COR, Lincoln, NE, USA). The standard verification measures were applied, including linear detrending, correction of low-pass (Moncrieff et al., 1997) and high-pass (Moncrieff et al., 2004) filtering effects, covariance maximization and WPL correction for density fluctuation (Webb et al., 1980). Coordinate rotation of wind speed was performed using a sector-wise planar fit approach (Wilczak et al., 2001) and removed spikes in the high-frequency data (Vickers and Mahrt, 1997). Fluxes were quality flagged using the EddyPro flags method according to the steady-state test as well as the test for developed turbulent conditions and combined into a 0–1–2 quality system (Mauder and Foken, 2004).

The resultant 30 min fluxes of energy and H_2O were subject to post-processing using Tovi software (LI-COR, Lincoln, NE, USA). Biometeorological data merge and gap-filling were done on a monthly basis with measured meteorological data and external data (BOM, 2021). Soil heat flux storage correction was done to improve the energy balance closure and compute the storage of energy between the soil surface and the soil heat flux plate (Tanner and Fuchs, 1968). Failure to account and correct for heat storage in the soil

above the plate can result in large errors that would lead to a subsequent underestimate of the latent heat (LE) and sensible heats (H) (Ochsner et al., 2006). The EC results were subject to further filtering under conditions of stable stratification and low turbulent mixing (primarily during the night), and a routine criterion for the friction velocity (u*) was applied on a seasonal basis for two years via the moving-point test (Papale et al., 2006). The threshold values for friction velocity were: 0.238 (SD 0.046) winter, 0.177 (SD 0.037) spring, 0.221 (SD 0.04) summer and 0.332 (SD 0.068) autumn.

The footprint or area sampled by the flux tower was determined using the Kljun et al. (2015) footprint model. This estimates the degree to which measured fluxes represent the peatland surface and to what extent they are affected by fluxes from the upwind grassland or other surfaces for each 30 min period. The assessment showed that the average contribution distance, accounting for 80% of flux, was 107 m (Fig. 1b). The site evaluation approach described by Göckede et al. (2008) was adopted to assess the spatial representativeness of the flux measurements using a four-group classification. This analysis showed that 67% of data exceeded an 80% threshold contribution from the peatland and were therefore categorized as "acceptable measurements". This approach was also applied to each season, wherein we found "acceptable measurements "occurred 71% of the time in spring, 69% summer, 75% autumn and 65% of the time in winter. Fluxes from adjacent non-target land covers (grassland and woodland) were filtered from the data set. The marginal distribution sampling (MDS) method was used for gap-filling to prevent underestimation of EC based evapotranspiration (ET_{EC}) in the subsequent calculation of daily averages and monthly and seasonal sums of evapotranspiration (Reichstein et al., 2005). This method is a moving window average method and considers both the co-variation of fluxes with meteorological variables and the temporal auto-correlation of the fluxes.

2.4. Fluxes and energy balance calculations

The 30 min mean fluxes and energy balance calculations are described in Supplementary Material. We follow the Euroflux methodology of Aubinet et al. (1999).

2.5. Reference evapotranspiration and ecosystem-soil-vegetation coefficient

The ET_{EC} was used to calculate an ecosystem-soil-vegetation coefficient (K_{ESV}), using an application of the FAO crop coefficient model, whereby we modified the initial model such that K_{ESV} is the ratio between ET_{EC} (mm h^{-1}) and ET_O (mm h^{-1}). Under environmental conditions, peatland vegetation may be stressed due to a lack of soil moisture, and thus ET_{EC} can be lower than ET_P, and this would influence the K_C. Hence we use K_{ESV} as a combined coefficient that parameterizes evapotranspiration not simply from a single crop species, as in the original K_C, but from the whole ecosystem, including soil and multiple species of vegetation in the peatland ecosystem. The ET_O was computed following the Penman-Monteith reference evapotranspiration approach outlined by Allen et al. (1998).

Satellite data for the leaf area index (LAI) of the peatland was acquired from the Oak Ridge National Laboratory Distributed Active Archive Centre (https://daac.ornl.gov/). LAI is a dimensionless parameter defined as the one-sided photosynthetically active area in the canopy per unit ground area. LAI data is available for flux tower sites around the world as the product of MODIS fixed sites subsetting and visualization tool (ORNLDAAC, 2018).

2.6. Peatland hydrology and ionic ratios

Stream water discharge was measured at 30-minute intervals at a gauging weir (90° v-notch; 300 mm) at the peatland drainage point (peatland 'exit') with water height recorded using a Trutrack water height logger (WT-HR 500; TruTrack Ltd, Christchurch, New Zealand). The water table depth (WTD) in the peatland was monitored with 5 piezometers installed into the underlying substrate. These piezometers were installed in a transect running between the major groundwater source for this peatland and the gauging weir and spaced at 50 m intervals (see: Karis et al., 2016). Piezometers comprised perforated 32 mm PVC tubing protecting 1-metre Trutrack water height loggers (WT-HR 1000). All loggers were configured to read at 30 min intervals, and data transfer was carried out using Omni7 software (Trutrack Ltd, Christchurch, New Zealand). Manual readings of weir stage heights were taken for calibration of logger heights.

Water sampling was conducted at 2 – 4 monthly intervals over the 2-year study period as part of a long-term monitoring program. All sampling was conducted under base-flow conditions, the criteria for which were: more than seven days after an event of greater than 25 mm, as informed by previous long-term patterns and event studies at this site (Silvester, 2009; Karis et al., 2016). Water samples were collected from both the major groundwater source (feed) and weir overflow (exit) for quantification of physical parameters as well as a range of dissolved components (see: Silvester, 2009 for analytical details). Included in the long-term monitoring program analytes are major cations (Na^+, K^+, Ca^{2+}, Mg^{2+}) and major anions (Cl^-, NO_3^-, SO_4^{2-}) as well as buffering components (HCO_3^-, dissolved organic carbon). In this work, we use only a subset of the major ions (Cl^-, Na^+, Ca^{2+}, Mg^{2+}) collected for the long-term program. The rationale for this selection was: (i) ions that are more commonly used for ET measurement (e.g. Cl^-) (Cook and Herczeg, 2012) and ions that exhibit seasonal patterns in this systems that are consistent with ET control (Ca^{2+} and Mg^{2+}) (Silvester, 2009).

The following equation can describe the water balance in this peatland:

$$\Delta V = P_n + G_i - ET - S_o - G_o \quad (1)$$

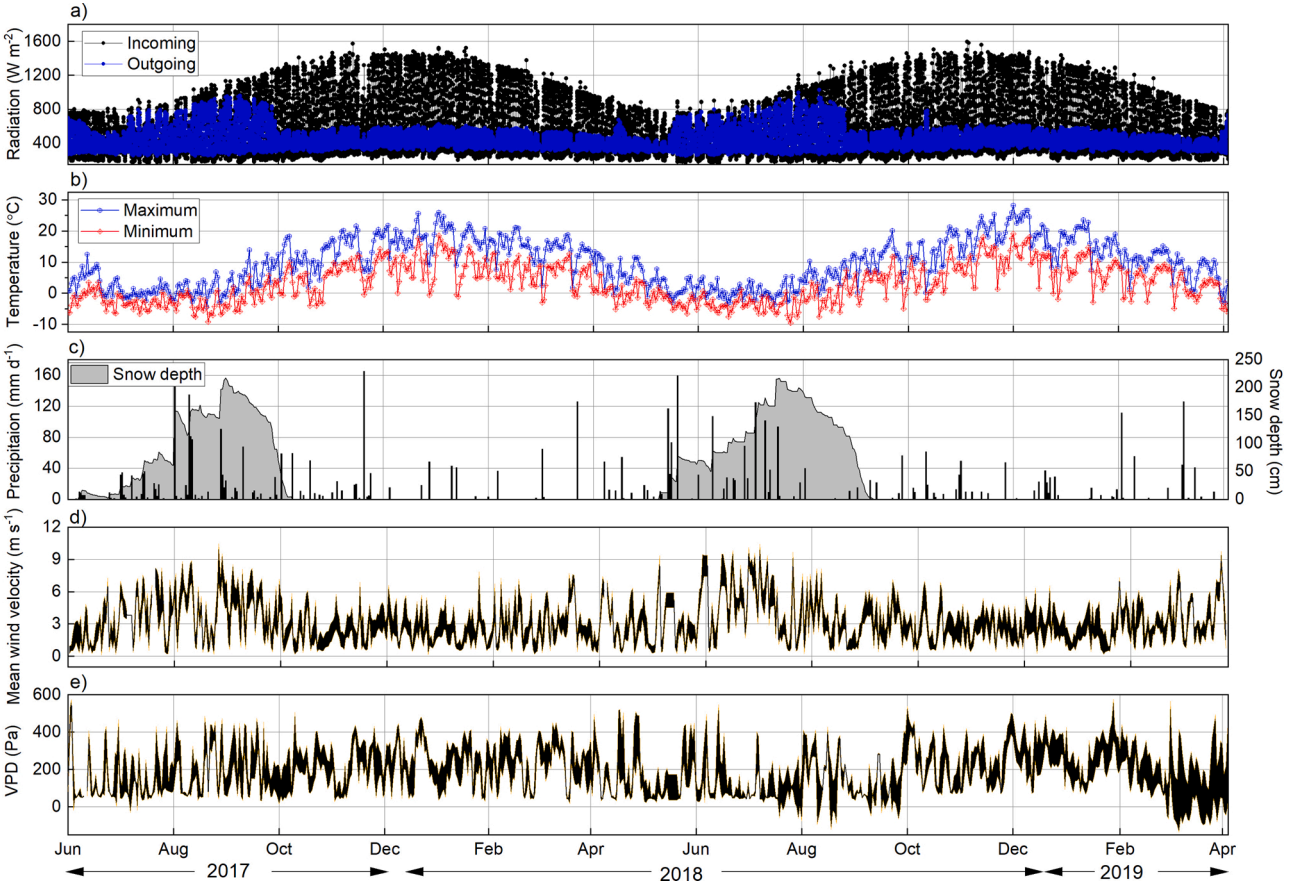

Fig. 2. Selected environmental variables at AU APL: (a) incoming and outgoing radiation; (b) maximum and minimum air temperature; (c) daily precipitation (BOM) and winter snow depth (Falls Creek Resort); (d) daily mean wind speed; (e) vapour pressure deficit (VPD). Shaded areas in (d) and (e) represent the daily minimum and maximum variations in these variables.

where ΔV is the change in water storage in the peatland, P_n is the net precipitation, G_i is groundwater inflow, ET is evapotranspiration, S_o is the surface outflow (peatland drainage) and G_o is groundwater outflow. Under the base flow conditions used here for water sampling, both ΔV and P_n are negligible, allowing groundwater inflows (Q_{feed} ($\approx G_i$)) to be calculated from peatland drainage (Q_{exit} ($\approx S_o$)) and ET using the aerial extent of the peatland (5.2 ha.), provided that the groundwater outflow (G_o) is negligible; this is a reasonable assumption as permeability is very low in the deeply humified peat zone.

In this work, 5-day running averages for both ET_{EC} and Q_{exit} were used, consistent with the base-flow criteria. For an ionic species controlled by water loss through evapotranspiration (i.e. conservative), the composition of peatland drainage water relative to groundwater feed is then given by equation 9.

$$\frac{[Ion]_{exit}}{[Ion]_{feed}} = \frac{Q_{feed}}{Q_{exit}} \tag{2}$$

The key assumptions of this model are: (i) no ion loss through evapotranspiration and (ii) that the groundwater composition from the major groundwater source is representative of all groundwater inputs into this peatland. Deviations from conservative behaviour can be attributed to peatland biogeochemical processes (e.g. dry deposition, mineral dissolution, plant uptake or microbial nutrient cycling). Ion ratios above that expected from ET water loss indicate net export from the peatland, while ion ratios less than that expected from ET water loss indicate biogeochemical retention or sequestering mechanisms.

2.7. Statistical analysis

Univariate ANOVA was used to analyse the significance of the temporal changes in measured and calculated parameters. The degree to which environmental variables controlled evapotranspiration was analysed by stepwise multiple linear regression (MLR). The parameters of MLR equations were estimated assuming that ET_{EC} was the dependent variable and the environmental variables were independent variables. The two-year study period was divided into seasonal blocks to allow inter-seasonal comparisons. All the statistical analyses were performed on the 24-h average values or daily ET values using the SPSS 25.0 program for Windows (SPSS Inc., Illinois, USA). Hydrologic and ionic data were manipulated in R and plotted using ggplot2 (RStudio Team, 2015).

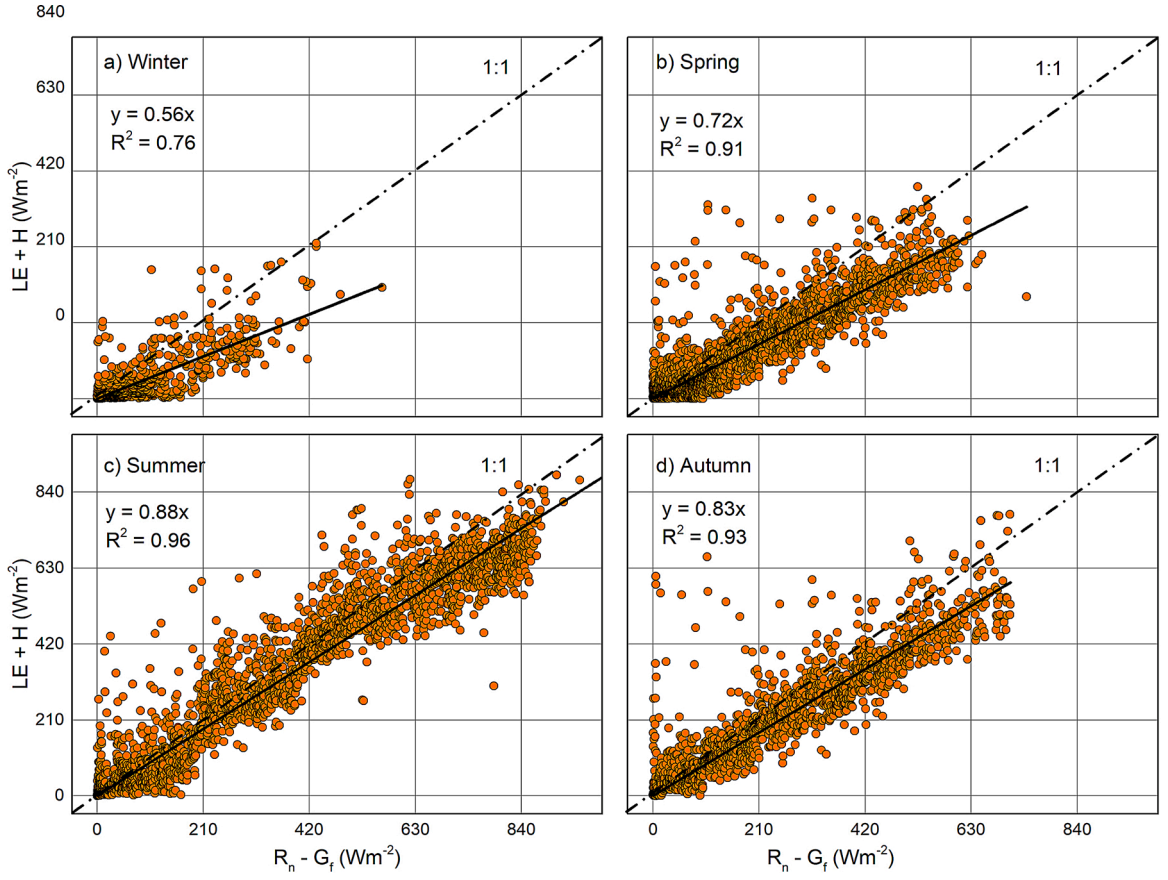

Fig. 3. Energy balance closure for the EC system in winter, spring, summer and autumn, as represented by the regression slope between the available energy ($R_n - G_f$) and the turbulent fluxes (H + LE).

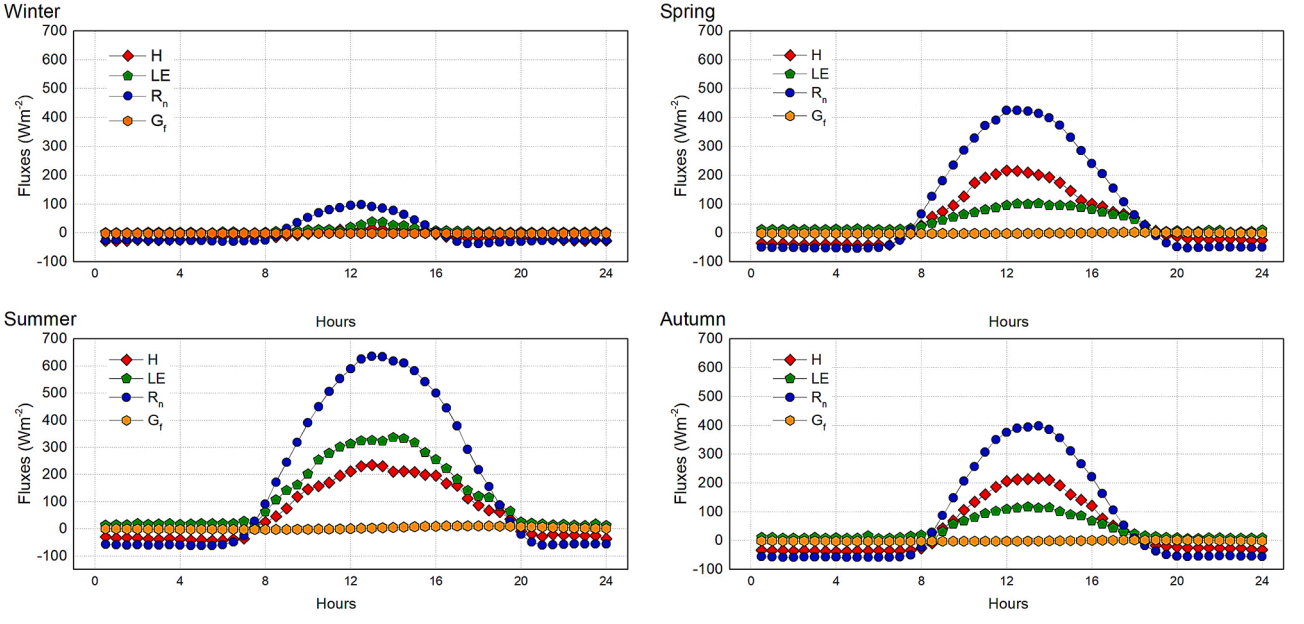

Fig. 4. The seasonal variations of energy fluxes for 24-h ensembles for winter, spring, summer and autumn. Fluxes shown are net radiation (R_n), sensible heat flux (H), latent heat flux (LE) and ground heat flux (G_f).

3. Results

3.1. Environmental variables impacting upon ET

Primary meteorological variables were collected from June 2017 to May 2019, providing two years of continuous measurements (Fig. 2). Incoming solar radiation was generally consistent year-round, with the mid-day average (10.00 – 14.00) higher in summer (1426 wm^{-2}) and lower in winter (773 wm^{-2}) (Fig. 2a). The annual pattern of incoming and outgoing radiation showed seasonal dynamics, with the outgoing solar radiation nearly two times higher in winter than in other seasons due to the high albedo of the snow cover. Air temperature followed the pattern of incoming solar radiation, and the mean annual maximum temperature was 9.5 °C, while the mean annual minimum temperature was 2.7 °C (Fig. 2b). Total rainfall for the two study years was 1976 mm and 2244 mm, respectively (BOM, 2021). The majority of precipitation in the Australian Alps falls as snow, and the major snowfalls occur between June and October (Fig. 2c) (Williams, 1987). During the measurement period, low wind speeds prevailed with a mean wind speed of 3.53 m s^{-1} and the maximum wind speed of 13.42 m s^{-1} (Fig. 2d). The highest wind speeds were recorded in winter as a consequence of reduced surface friction due to snow cover. The vapour pressure deficit (VPD) was generally low during winter (less than 5 hPa), indicating near-saturation of the air with water vapour, while higher average daily VPDs were observed in spring and summer periods. Summer, in particular, was characterized by extremely low humidity with several days having very high VPDs.

3.2. Energy fluxes and balances

3.2.1. Energy balance closure (EBC)

Seasonal assessment of the energy balance closure (EBC) was used in this study to investigate potential uncertainties in the EC measurements and to understand how these may vary through the year. The surface energy balance is fundamental for all atmospheric interactions, and balance is a theoretical requirement of the first law of thermodynamics. EBC is tested by statistically regressing the sensible and latent heat fluxes against the available surface energy, and the ideal EBC would be achieved when the slope of the linear regression is unity (Li et al., 2005). The linear regression relationship between the turbulent fluxes (H + LE) and available energy (R_n – G_f) resulted in an EBC (slope) of 0.72, 0.88, 0.83 and 0.56, with the coefficient of determination (R^2) of 0.91, 0.96, 0.93 and 0.76, for spring, summer, autumn and winter (Fig. 3). The most complete EBC was observed in the summer season, corresponding to the highest flux period of the year, decreasing into spring, autumn and winter. During low flux times of the year, EBC is more variable, unpredictable, and tends to be smaller. Our results were within the typical closure achieved for EC, which ranges from 70 to 90% for most ecosystems (Poyda et al., 2017), except in winter when snow cover and low flux decreased the EBC to 0.56.

3.2.2. Seasonal changes in energy fluxes

The mean hourly energy fluxes for 24-h periods in each season (averaged across both years) are commensurate with the site's alpine location within the sub-polar oceanic Köppen (Cfc) climate zone (Fig. 4). Day length is notably longer in summer (14.7 hrs) compared to winter (10.1 hrs). Comparatively, the daily global solar exposure has its highest monthly mean in January (25.2 MJ m^{-2}) and lowest monthly mean in July (5.4 MJ m^{-2}) (BOM, 2021). There is also a much greater range in the incoming solar radiation (R_n) in summer than in winter (summer: −60 Wm^{-2} to 630 Wm^{-2}; winter: −30 Wm^{-2} to 100 Wm^{-2}). This incoming solar energy drives changes in latent heat (LE), sensible heat (H) and ground surface temperatures (G_f), the partitioning of which varies by season.

In summer, LE > H (Fig. 4) and this is reflected in a Bowen ratio (β = H/LE) <1 and evapotranspiration fraction (EF = LE / (LE+H)) > 0.5 (Table 1), indicating a large fraction of available energy was used for evapotranspiration. In spring and autumn, this pattern is reversed, with H > LE (Fig. 4), β of > 1 and EF < 0.5. All energy flux components were low and variable in the winter (Fig. 4), and so β and EF for this season should be interpreted with caution. Diurnal variations in G_f are very low, albeit 10-fold greater in summer compared to winter (Fig. 4), but at all times, G_f is a minor component of the overall energy balance.

3.3. Evapotranspiration and ecosystem-soil-vegetation coefficient

Evapotranspiration (ET_{EC} and ET_O) show clear seasonal patterns (Fig. 5a). The overlap between measured and estimated values is excellent except in spring (Sept-Oct) when ET_O is often greater than ET_{EC} and a few days in summer when ET_{EC} is greater than ET_O. Seasonal daily average values of ET_{EC} were: 0.38, 1.37, 3.29 and 1.32 mm day^{-1} for winter, spring, summer and autumn, respectively.

Table 1
Average daytime (10.00 – 14:00) flux ratios for each of the seasons (for each of the two year periods from June 2017 to May 2019). Listed are the partitioning of nett radiation towards sensible heat (H/R_n) and latent heat (LE/R_n), the Bowen ratio (β) and the evapotranspiration fraction (EF). (R_n = net radiation, LE = latent heat, H = sensible heat).

Season	H/R_n		LE/R_n		β = H/LE		EF = LE/(LE+H)	
	2017/18	2018/19	2017/18	2018/19	2017/18	2018/19	2017/18	2018/19
Winter	0.22	0.23	0.30	0.32	0.41	0.45	0.72	0.75
Spring	0.5	0.48	0.21	0.23	2.1	2.2	0.32	0.33
Summer	0.35	0.36	0.51	0.54	0.71	0.73	0.57	0.61
Autumn	0.53	0.55	0.28	0.29	1.89	1.83	0.34	0.35

The mean ecosystem-soil-vegetation coefficient (K_{ESV}) for the peatland, which is the ratio between ET_{EC} and ET_O, was 0.78 with an R^2 value of 0.84 (Fig. 5b); this strong correlation deviates considerably from 1 at low ET_{EC} values. Cumulative ET curves (Fig. 5c) show that both ET_{EC} and ET_O in 2017/18 were lower than in 2018/19 and also confirms the close agreement between measured (ET_{EC}) and estimated values.

3.4. Seasonal changes in the ecosystem-soil-vegetation coefficient and LAI

The K_{ESV} showed apparent seasonal variation, which mirrors the changes in the leaf area index (LAI) of the ecosystem (Fig. 6). K_{ESV} values ranged between 0.5 in early spring directly after snowmelt up to a maximum of 1.1 in mid-summer. Similarly, LAI varied between 2 in early spring and 3.75 in mid-summer. Given that this is a highly seasonal ecosystem with winter snow cover, we define three stages of vegetation growth: October – November (early growth season), December - February (peak growth season) and March-May (senescence). These growth stages are clearly evident in the LAI profiles, with distinctly higher values during the peak growth season (~3.5) compared to either early growth or senescence (~2.0 – 2.5). Both K_{ESV} and LAI were lower in 2017/18 compared to 2018/19.

3.5. Water table depth and evapotranspiration

The water table depth (WTD) in the peatland showed a clear annual cycle over the two-year study period (Fig. 7), with maximum WTD occurring during spring and soon after snowmelt. The yearly range in WTD was ~400 mm in 2017/18 and ~300 mm in 2018/19. During non-snow cover periods (Oct-May), short-term spikes in WTD of up to 300 mm were observed corresponding to rain events. These increases in WTD represent the hydraulic buffering provided by the peatland and decayed to pre-event levels over less than one week. WTD and ET_{EC} were effectively out-of-phase with each other, with maximum ET_{EC} occurring in mid to late-summer and corresponding to the period of declining WTD. An exceptionally dry period occurred during summer 2017/18, leading to very low WTD (see: highlighted region Feb-Mar 2018) and corresponding with particularly low values of ET_{EC} (average value 0.6 mm d^{-1} was

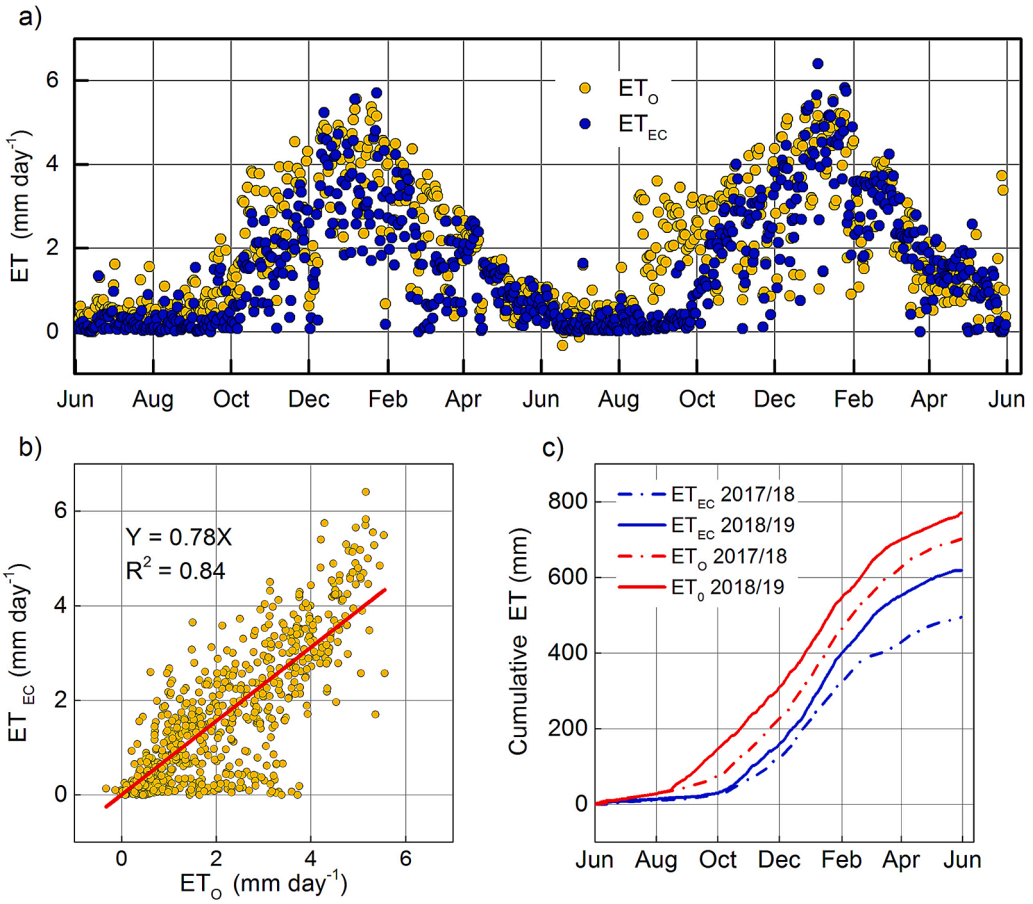

Fig. 5. (a) Daily total evapotranspiration for the two years June 2017 to May 2019; (b) correlation of actual evapotranspiration (ET_{EC}, mm d^{-1}; measured via eddy covariance) against reference evapotranspiration (ET_O, mm d^{-1}) yielding the ecosystem-soil-vegetation coefficient (K_{ESV}); (c) cumulative measured (ET_{EC}) and reference evapotranspiration for full-year periods: 2017/18 and 2018/19.

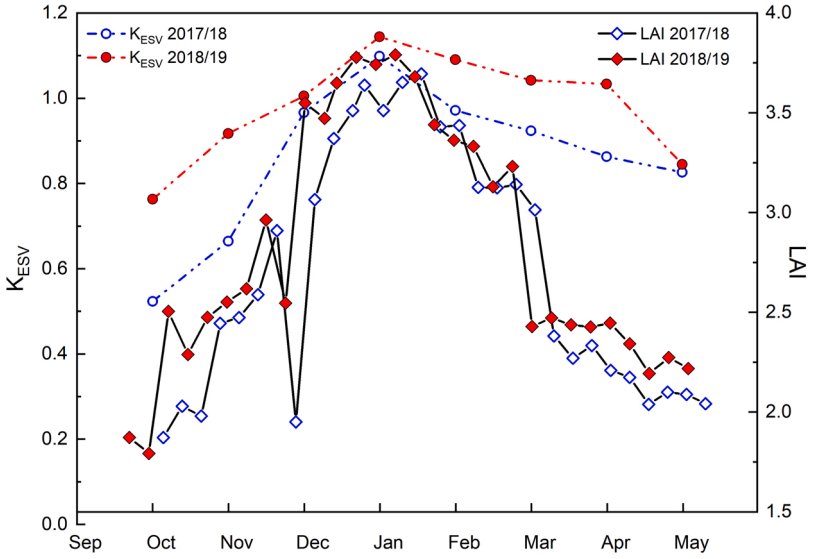

Fig. 6. The mean monthly ecosystem-soil-vegetation coefficient (K_{ESV} dashed lines) and MODIS LAI (solid lines) for the snow-free periods of 2017/18 and 2018/19.

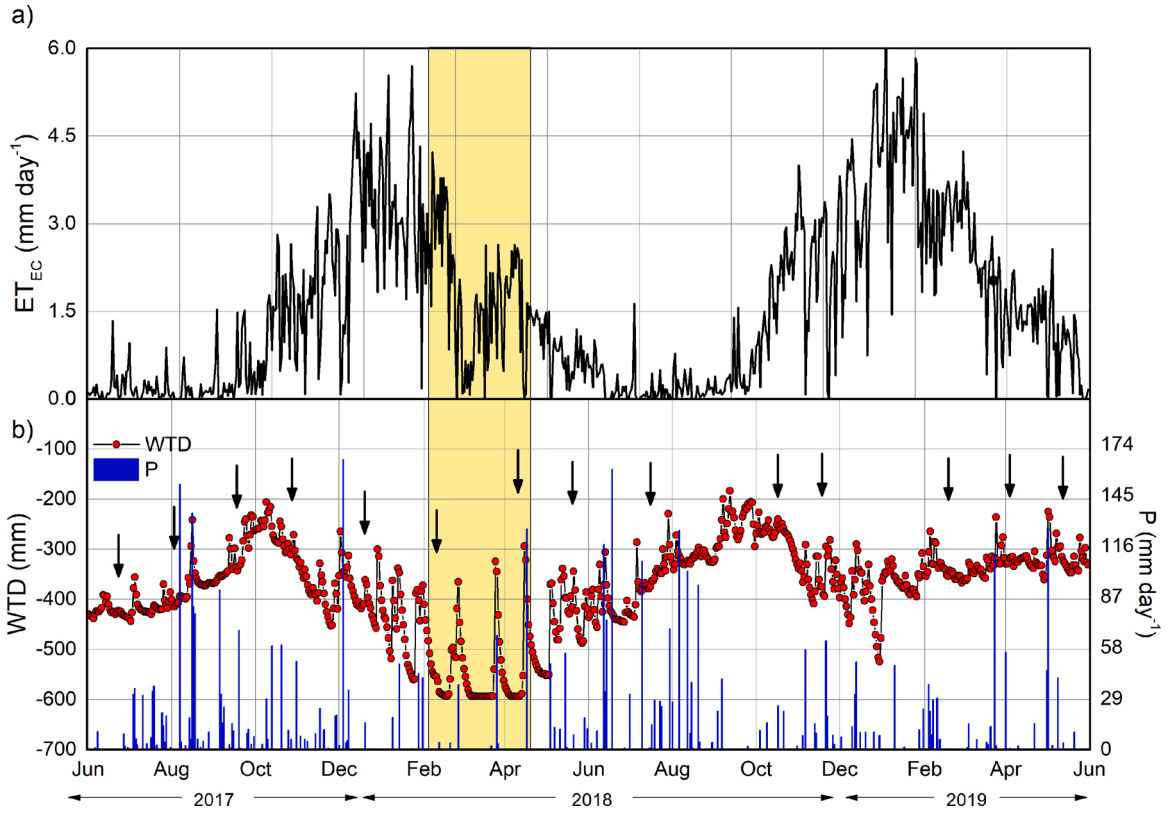

Fig. 7. Mountain peatland ecohydrology: (a) evapotranspiration (ET_{EC}); (b) water table depth (WTD, referenced to peatland surface) and precipitation (P). Arrows in (b) are water sampling occasions for the ionic composition of groundwater and peatland discharge (stream) water.

recorded for two weeks). Importantly, the estimated fraction of precipitation lost from the peatland through evapotranspiration (ET_{EC}/P) is 0.25 in 2017/18 and 0.28 in 2018/19 and suggests an exceptionally high transfer of precipitation to run-off.

3.6. Relationship between ET_{EC} and environmental drivers

Potential relationships between ET_{EC} and measured environmental variables were explored by single parameter linear regression and multiple linear regression (MLR). Variables considered in this analysis were: net radiation (R_n), air temperature (T_a), vapour pressure deficit (VPD) and water table depth (WTD). R_n was the environmental variable with the highest single-parameter correlation to evapotranspiration (R^2 = 0.86 and 0.92 for 2017/18 and 2018/19, respectively) (Figure S1a). T_a and VPD were also strongly predictive of ET_{EC} (T_a: R^2 = 0.8 and 0.91 for 2017/18 and 2018/19, respectively; VPD: R^2 = 0.80 and 0.77 for 2017/18 and 2018/19, respectively) (Figure S1b, S1c).

Consistent with single parameter regressions, MLR identified R_n, T_a and VPD as strong and significant predictors of ET_{EC} over the entire two-year period (Table S1; R^2 = 0.8; $p < 0.01$ (R_n and T_a); $p < 0.1$ (VPD)). MLR for individual seasons similarly identified these three environmental variables as the best predictors of ET_{EC} in spring and summer (Table S1). For the winter periods, none of the environmental variables showed a strong correlation with ET_{EC}, likely due to snow cover over the peatland. During autumn, VPD was not significantly correlated with $ET_{EC,}$ but instead, WTD, R_n and T_a were identified as significant driving variables. The predictive power of these variables, however, varied between years and was substantially less in autumn 2018 (R^2 = 0.34) compared to autumn

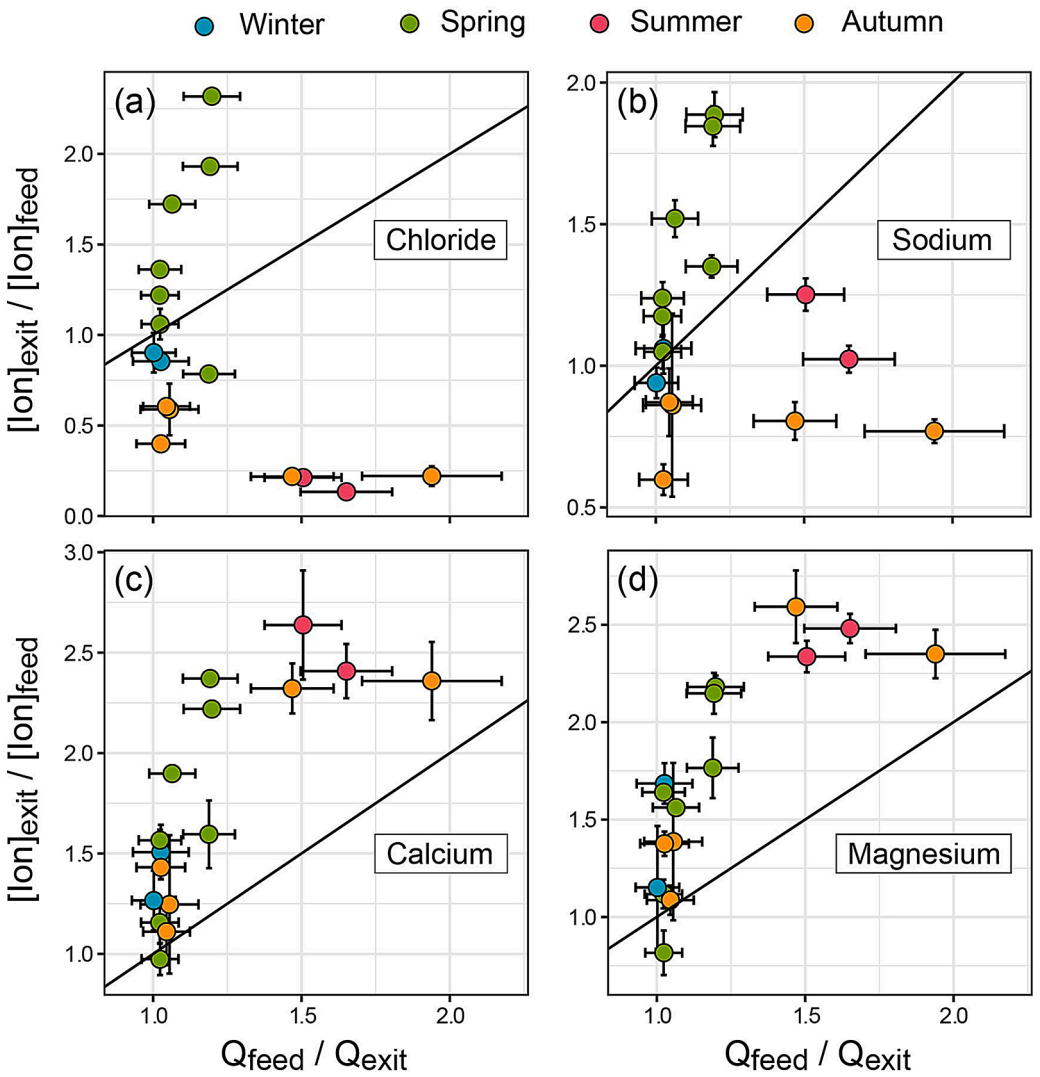

Fig. 8. Ion ratios for peatland exit and groundwater feed ($[Ion]_{exit}/[Ion]_{feed}$) plotted against Q_{feed}/Q_{exit} for samples collected under base-flow conditions over the two-year study period; Q_{feed} calculated from 5-day averaged values of ET_{EC} and Q_{exit}. Shown are: (a) chloride, (b) sodium, (c) calcium and (d) magnesium. The solid line represents the expected response for a conservative ion controlled by water loss through evapotranspiration. Error bars for ion ratios are ±2SE, while error bars for discharge ratios are based on height error of 2 – 5 mm in weir readings.

2019 ($R^2 = 0.76$). WTD was a strong and significant predictor of ET_{EC} only in spring ($p < 0.001$).

3.7. Ion ratio comparison with ET_{EC}

The major ion composition of groundwater (peatland feed) and stream water (peatland exit) was measured on a 2 – 4 monthly frequency over the two years of the study (sampling occasions are shown in Fig. 7). This sampling was always conducted under base-flow conditions, under which the ratio of ion concentrations in peatland exit water to peatland feed ($[Ion]_{exit}/[Ion]_{feed}$) should be equal to the inflow and outflow ratio (Q_{feed}/Q_{exit}) for ions that behave conservatively (solid line in Fig. 8). Here we have used the Q_{exit} values from 5-day averaged weir plate logger data which were very similar to manual readings recorded at the time of water sampling, consistent with base-flow conditions (Figure S2).

Both Cl^- and Na^+ behaved in similar ways to each other across the two years with a net export of ions during spring and retention during summer and autumn (Fig. 8a, b); this ion retention was somewhat stronger for Cl^- than Na^+. For both ions, the winter ion ratio was approximately one as expected for this snow-covered period when ET is low and is consistent with the assumption that the groundwater source sampled for this work is representative of all groundwater inputs; under this condition, there are effectively no water loss or peatland regulation processes operating, so the ionic compositions of feed and exit waters converge. Overall the patterns observed for Cl^- and Na^+ suggest a post-snow melt release of these ions followed by a more extended period of ion retention and generally mirror seasonal behaviours previously observed for these ions in this system (Silvester, 2009). Ion ratios for Ca^{2+} and Mg^{2+} were also similar to each other and distinctly different to Cl^- and Na^+. For both Ca^{2+} and Mg^{2+}, net export was observed in all seasons, approaching that predicted for a conservative ion at both low and high values of Q_{feed}/Q_{exit} (Fig. 8c, d). At low $Q_{feed}/Q_{exit,}$ this could be due to reduced biogeochemical reaction rates during winter snow cover months, similar to Cl^- and Na^+. The net export of these ions outside of winter months suggests a source of these ions within the peatland, such as a mineral dissolution or ion exchange process. The similar behaviour of Ca^{2+} and Mg^{2+} in peatland exit water is consistent with the constant Ca: Mg ratio (~1:2 molar ratio) previously observed across both seasonal and event timescales (Silvester 2009; Karis et al., 2016).

4. Discussion

Very few EC flux measurements exist for peatlands in mountainous regions due to a range of challenges in measuring surface-atmosphere exchanges under these conditions (Xu et al., 2018b, Gerling et al., 2019). In particular, landscape heterogeneity has a substantial influence on the measurement and interpretation of atmospheric data (Schmid and Lloyd, 1999, Schmid, 1997), and peatlands in mountainous regions are typically heterogeneous landscapes. Since for most tower sites, the extent of horizontal variation is 1 km or less, the scale of horizontal homogeneity will be exceeded by the fetch of the flux measurements (Jegede and Foken, 1999, Göckede et al., 2008). It is therefore critical that a footprint analysis is performed to test whether the 'spatial representativeness' assumptions in the EC method are valid (Schuepp et al., 1990, Horst and Weil, 1992, Schmid, 2002, Leclerc et al., 1997, Rannik et al., 2000, Kljun et al., 2004, Kljun et al., 2015). This study demonstrates that it is feasible to acquire ecosystem-level ET measurements with the EC approach at this mountainous peatland site, even with a restricted fetch and heterogeneous surface characteristics. This has been achieved by careful consideration of tower placement, including prior knowledge of wind direction, low installation height, adopting a rigorous footprint analysis, performing adequate corrections, and following standard filtering. The flux tower at this peatland site (AU-APL) produced a valid data set for 72% of the two years study period after rigorous QA/QC, suitable for further investigation of ET. We demonstrate that in small alpine mountainous peatlands, the EC technique provides well-validated datasets for further ecohydrological analyses.

4.1. Seasonality and energy balance

A number of individual sites within the FLUXNET network use energy balance closure (EBC) as a standard procedure to assess flux data quality (Li et al., 2005). Our study results suggest that the closure of the energy balance was strongly connected with seasonal variations. While the energy fluxes measured by the EC system were not completely closed, the mean EBC (0.78) of the EC measurements was acceptable. Spring, summer, and autumn EBCs (72% – 88%) were consistent with previously reported results, ranging from 53% to 99% for FLUXNET sites (Li et al., 2015). Lower EBC during winter has also been reported in other long-term studies using eddy covariance (Li et al., 2015) and seasonal evaluation of ET and energy budgets (Deb Burman et al., 2019). The low EBC during winter is likely caused by a low signal to noise ratio in flux measurements (Stannard et al., 2013) combined with the effects of melting and freezing, which were not considered in energy balance evaluation (Li et al., 2005). However, in this study, the winter season is considered a non-growing season, and the winter season energy budget makes a relatively small contribution to the yearly energy balance (Wu et al., 2010). Across all seasons, EBC values less than one suggests an underestimation of the sensible heat (H) and/or latent heat (LE) fluxes. Applying the energy balance closure adjustment of De Roo et al. (2018) (Section 2.3) corrects the eddy-covariance measurements of H and LE and improves the overall EC-derived ET estimation.

Sensible heat flux dominated the energy partitioning during the spring and autumn seasons, with less energy directed towards LE. During summer, LE was larger than H, corresponding with high incoming solar radiation, as illustrated by Fig. 2. Consistent with the seasonal variations in energy partitioning between H and LE, β values varied over a wide range (0.42 to 2.2) over the two-year study period. A similar seasonal pattern was observed in marshland areas in the Central United States (Lenters et al., 2011) and in multi-season measurements in wetlands in north-eastern China (Zhou and Zhou, 2009). Gerling et al. (2019) showed that the seasonal variation of β is inversely related to the variation in VPD. VPD increases exponentially with atmospheric temperature, leading to lower

β values during summer (Hirano et al., 2016, Shimoyama et al., 2003, Majozi et al., 2016). The concurrence in the above studies, including this one, is that vegetation dynamics play a crucial role in energy partitioning and that in summer, with during l vegetation cover, LE flux is the dominant portion of net radiation.

4.2. Evapotranspiration and run-off

Our observations over two complete years contribute significantly to the understanding of mountain peatland evapotranspiration characteristics and their response to hydro-meteorological changes. A hydrological modelling study of the 335 ha Watchbed Creek catchment (that this peatland forms part of) suggested that the estimated annual potential ET was 558 mm, averaged over the years 1940 – 1986, with the highest values during summer (January PET = 145 mm) and lowest in winter (June PET = 35 mm) (Western et al., 2008). Our average annual ET_{EC} of 556 mm for a peatland in this catchment appears reasonable when compared with other *Sphagnum* dominant peatland ecosystems under similar synoptic weather conditions. For example, Cao et al. (2020) observed that the annual ET in an alpine wetland ecosystem in Qinghai on the Tibetan Plateau was 644 mm/year; Petrone et al. (2001) showed a growing season average ET in restored peatlands in Quebec of 354 mm; Wu et al. (2010) found the ET of boreal peatlands in eastern Finland to be 321 mm, and Hirano et al. (2016) measured the ET of Sarobetsu Mire (Japan) to be 372 mm. Similarly, Gerling et al. (2019) reported a maximum ET of 5.6 mm d^{-1} for an ombrotrophic peat bog in Central Germany and Lafleur et al. (2005) recorded maximum ET rates at a peatland in Ontario, Canada ranging over 4 – 5 mm d^{-1}, similar to the summer ET_{EC} of this study.

Synoptic weather conditions (i.e. air temperature, vapour pressure deficit and incoming solar radiation) could explain differences in ET_{EC} among the seasons and between study years (Table S1 and Figure S1). Consistent with this, our study shows that evapotranspiration is a function of R_n, T_a and VPD, while it is inversely proportional and weakly correlated with WTD (Figure S1). However, differences were observed between seasons, with spring, summer and autumn showing the strongest correlations with these environmental factors. Cumulative ET data (Fig. 5c) show that annual ET in 2018/19 was higher than in 2017/18, which we attribute to a low rainfall period during February- March in 2017/18, resulting in an exceptionally low water table. This result is different to that observed by Moore et al. (2013), where short-term water table variation did not control ET in a peatland ecosystem. Very few other studies have characterised interannual variability of ET in relation to changes in moisture availability (Lafleur et al., 2005, Liljedahl et al., 2011). The reduced ET at extremely low water table depths may be due to the absence of any mechanism for the transportation of water from deeper in the peat profile; the dominant *Sphagnum* moss has no stomata, roots, or water-conducting tissues, so vertical water transport may be limited (Shimoyama et al., 2003).

The ecosystem-soil-vegetation coefficient (K_{ESV}) approach applied in this study provides evidence of a strong relationship between ET_{EC} and $ET_{O,}$ and this coefficient, as determined separately for each season, can effectively be used in ecohydrological studies of other mountain peatlands with similar vegetation. K_{ESV} values determined for each season were: 0.68 spring (early growing season), 1.12 summer (peak growing season) and 0.88 autumn (senescence). The K_{ESV} obtained for this peatland were in a similar range to that reported for ombrotrophic peat bog Odersprungmoor in the Harz Mountains, Central Germany (K_C in the range: 0.82 - 0.86) (Gerling et al., 2019). In the Australian mountains, the spring season is potentially the most sensitive to the difference between ET_{EC} and ET_O because some of the available energy in the peatland is likely used to heat the standing water. Once the standing water in the peatland has heated, more of the net radiation (R_n) is directed towards H and LE (Drexler et al., 2008). Seasonal variation in the effective leaf area coverage and photosynthetic capacity of the vegetation, described by LAI and which are only relevant outside the snow cover season, display a similar trend to the K_{ESV}. In the early growing season, the reduced leaf development after snowmelt coincided with lower K_{ESV}, while both parameters were highest in mid-summer, corresponding to the peak growing season. The strong seasonal variability in K_{ESV} values obtained in this work suggests that the use of a single K_{ESV} is not appropriate in mountain peatlands.

This region experiences high precipitation, and our work suggests that the average net evapotranspiration is 26.5% of the precipitation. The remaining portion of precipitation is presumably contributing to catchment run-off. Consistent with this, Western et al. (2008) showed through hydrological modelling analysis that the average run-off coefficient for the entire Watchbed Creek catchment (335 ha), including this study area, was 0.77. Further, Lawrence (1995) proposed that for the Watchbed Creek catchment, 67% of effective precipitation appeared in streams as quick-flow, for effective precipitation values between 0.9 and 4.5 mm, while 40% of effective precipitation appeared in streams as quick-flow for effective precipitation values greater than 4.5 mm. Importantly, this suggests that the run-off potential is very high in the study area compared to elsewhere in the Australian landscape (Lawrence, 1995). Precipitation (and therefore run-off) is generally lowest at the end of summer (February/March), which leads to the lowering of the peatland water table. During this low rain period, the only significant inflows are from groundwater aquifers that provide sustained flow to these alpine aquatic ecosystems (McCartney et al., 2014). Climate change projections for the Australian Alps forecast decreasing snowpack (extent and depth) (Laurance et al., 2011, Pickering et al., 2004) which will likely impact groundwater recharge and affect the future viability of these peatland ecosystems.

4.3. Evapotranspiration and ion ratios

Seasonal patterns in nutrient and ion concentrations in peatland drainage water for this peatland have been described previously (Silvester, 2009). This previous work has shown strong uptake of nitrate and sulphate during warmer months and an atypical behaviour for Na^+ and Cl^- with apparent uptake of these ions during warmer high productivity periods. Among the major ions, only Ca^{2+} and Mg^{2+} show annual patterns in-stream concentrations consistent with water loss through ET. Here we confirm that strong ion retention (uptake) and export (release) mechanisms operate for Na^+ and Cl^-. While the net export of these ions could be due to a snowmelt flush, this effect continues well after snowmelt and does not explain the peatland uptake of these ions. Other possible

explanations are uptake and release associated with biological processes such as plant growth during high productivity periods followed by senescence or microbial uptake (e.g. organochlorine compounds (Bastviken et al., 2007)) and release. A key issue with both of these mechanisms is that the export of these ions occurs into late spring, whereas senescence (or microbial die-off) is more likely an autumn process. While we are unaware of similar seasonal uptake-release mechanisms for these ions in other wetlands, these processes may be more evident in this peatland due to the extremely low salt concentrations in the groundwater (Silvester, 2009). A significant result from the behaviour of Na^+ and Cl^- is that the ion ratio approaches a value of one (1) under low ET conditions. This is consistent with a key assumption of the model that the groundwater composition of the major source is representative of all groundwater sources into this peatland.

Ca^{2+} and Mg^{2+} concentrations approach that expected for a conservative ion at both high and low Q_{feed}/Q_{exit} but are always higher, indicating net export under all conditions. The approach to conservative behaviour at high Q_{feed}/Q_{exit} is consistent with previous observations for this system that ET calculated from Ca^{2+} and Mg^{2+} concentrations yield physically reasonable values under high ET conditions (1.7–2.5 mm d^{-1}) (Silvester, 2009; Silvester, 2009; Karis et al., 2016). The differences between observed and ET-predicted concentrations indicate additional sources of these ions from the peatland. Broadly these sources could include (dry) atmospheric deposition, the net loss of stored peat or mineral dissolution/exchange processes within the peatland. The pronounced seasonality of stream water Ca^{2+} and Mg^{2+} concentrations is a strong argument against dry deposition, the timing and loads of which are unlikely to be annually reproducible. The more compelling result is from storm response studies at this site (Karis et al., 2016) which show that both Ca^{2+} and Mg^{2+} concentrations are unaffected by high-intensity rainfall events; a significant dilution would be expected if these ions were controlled by dry deposition or peat soil decay. A mineral exchange or dissolution mechanism appears the most likely explanation of the observed behaviour where peatland drainage concentrations are controlled by a physical property of the peatland that is seasonally variable (e.g. temperature, water table, redox potential).

Overall, the observed seasonal patterns in uptake and release of ionic components confirm the strong controls on stream water composition (water quality) provided by these headwater peatlands. Given that both groundwater and rainfall contribute to the overall water budget, the seasonally reproducible regulation of peatland drainage water is likely a key function of these systems in the landscape.

4.4. *Implications for mountain peatland protection and rehabilitation*

Heathy Spur 1 (HS-1) is an intact Alpine *Sphagnum* peatland in the Bogong High Plains, Victoria, Australia, that serves as a reference ecosystem for understanding hydrological and biogeochemical functions of peatlands more broadly in this mountain landscape. Peatlands in the Australian Alps are highly restricted ecosystems, forming in hillside valley floors in close association with groundwater sources (McCartney et al., 2014). These ecosystems are highly likely to be stressed by future changes in precipitation regime from climate change. Understanding the water budget of these systems will be critical in predicting future trajectories for these systems and impacts on water yields from the Australian Alps. Quantifying the ET flux from this peatland and the climate factors that drive ET is an important component in developing a more complete water budget and separating the relative contributions of precipitation, snowmelt and groundwater in driving these ecosystems. Consistent with the high water yields from the Australian Alps, our data shows a low evaporation factor for this peatland, reflecting an environment with a substantial excess water yield to downstream catchments. Importantly, our results suggest that under extended low rainfall periods, ET may decrease due to disconnection between the water table and vegetation layer.

This study provides the first application of EC techniques to measure ET_{EC} and K_{ESV} in Australia's mountainous peatland ecosystems. Peatland restoration requires precise evapotranspiration estimates in order to successfully manage site hydrology (Holden, 2005). However, assessing actual evapotranspiration at each site is complex, costly and maybe impossible depending on the location, budget and time frame (Howes et al., 2015). For example, Australian alpine *Sphagnum* peatlands occur as a mosaic of many small peatlands within the wider landscape, and thus, direct measurement of evapotranspiration using EC at many sites is not possible due to landscape heterogeneity and slope. This study has determined K_{ESV} as a critical element of hydrological function, which has the possibility of wider applicability. The K_{ESV} values calculated in this study can provide a more accurate estimate of ET than traditional climate data-based approaches for other Australian alpine *Sphagnum* peatlands as well as peatlands in other areas with similar climatic conditions. Furthermore, the use of season-specific K_{ESV} values could contribute to improved accuracy in hydrological models from catchment to regional scales.

The delivery of large volumes of high-quality water is a key ecosystem service provided by the Australian Alps (Worboys and Good, 2011). Understanding the chemical regulation processes that occur in all hydrologic components, including those processes that occur at the top of catchments in peatland systems, is key to the long-term protection of this water quality. Previous work has demonstrated that drainage (stream) water quality is highly regulated in these peatland systems, both on seasonal as well as event timescales (Silvester, 2009, Karis et al., 2016). Since ET is a major component in the peatland water balance and a major driver of seasonal variations in drainage water concentration, the measurement of ET is a critical step in identifying peatland uptake and release processes. Our results show that these peatland biogeochemical processes show a strong seasonal patterning, most likely linked to peatland productivity and the generation of fixed carbon for microbial processes. We suggest these seasonal patterns are applicable across the Australian Alps for intact peatlands under similar synoptic weather conditions and could be used as part of a set of metrics to assess peatland condition and rehabilitation.

This study will be an effective tool for understanding the response of peatlands to changing climate and land management practices. Peatlands in this landscape are already in a range of conditions due to past land management practices (e.g. cattle grazing) and more recent disturbances (e.g. feral animal, weeds) that will likely impact resilience to future stressors. Understanding the hydrology and

linked biogeochemistry of these peatlands is integral to establishing favourable conditions for rehabilitation actions (Petrone et al., 2001).

5. Conclusions

Four main conclusions are drawn from this study:

1. Annual evapotranspiration from this peatland was 494 mm in 2017/18 and 618 mm in 2018/19, representing 26.5% of annual precipitation. ET_{EC} increased rapidly after snowmelt and reached maximum values in early summer. Winter ET_{EC} was 6.2% of the annual ET due to snow cover.
2. The K_{ESV} varied seasonally between 0.5 (spring and autumn) and 1.1 (summer). This study identified three distinct phenological stages in peatland productivity and suggested that the application of a single year-round K_{ESV} value is not appropriate in mountain peatland ecosystems.
3. This study revealed that evapotranspiration dynamics of the peatland are primarily influenced by net radiation, air temperature, VPD, and weakly influenced by water table depth (WTD). The exception is during severe drought periods when very low water table depth did correspond with reduced ET.
4. The measurement of ET reveals that for Cl^- and Na^+, the observed annual cycle is due to ion release and uptake, with net export in spring and net uptake in summer-autumn. For Ca^{2+} and Mg^{2+} net export occurs at all times of the year and indicates a seasonally dependent mechanism.

Author Contributions

MG, SG, ES Conceptualization; MG Data curation; MG, ES Formal analysis; SG Funding acquisition; MG, ES Investigation; SG, ES Methodology; SG ES Project administration; MG ES Visualization; MG, ES Roles/Writing - original draft; SG, ES, OJ Writing - review & editing.

Declaration of Competing Interest

The authors report no declarations of interest.

Acknowledgements

This research work was conducted under the provisions of Permit No 10008289, issued by the Department of Environment, Land, Water and Planning (DELWP). This research was financially supported by an Australian Government Research Training Program (RTP) Scholarship, administered by RMIT University, awarded to MG. The eddy-covariance flux tower was established by a La Trobe University “Securing Food Water and Environment Early Career Researcher” grant to SG. The authors wish to acknowledge the assistance of CSIRO for the loan of equipment essential for the flux measurements. We also thank Eva Van Gorsel, who was instrumental in establishing the AU-APL site and Steve Zegelin for supporting us in data collection, curation and flux tower maintenance. Data analysis was supported by Peter Isaac, Central Node, OzFlux, the Australian and New Zealand Flux Network. Instrument brand names are included to provide transparency around research protocol and do not constitute product endorsement. We acknowledge Andrew Kromar, Sean Keenan and Elaine Thomas from Parks Victoria for assistance in setting up the flux tower and ongoing help with its management. Further, we thank Falls Creek Alpine Resort for sharing their snow history reports.

Appendix A. Supplementary data

Supplementary material related to this article can be found, in the online version, at doi:https://doi.org/10.1016/j.ejrh.2021.100851.

References

Alberto, M.C.R., Wassmann, R., Hirano, T., Miyata, A., Hatano, R., Kumar, A., Padre, A., Amante, M., 2011. Comparisons of energy balance and evapotranspiration between flooded and aerobic rice fields in the Philippines. Agric. Water Manage. 98, 1417–1430.

Allen, R., Pereira, L., Smith, M., 1998. Crop evapotranspiration-Guidelines for computing crop water requirements-FAO Irrigation and drainage paper 56.

Aubinet, M., Grelle, A., Ibrom, A., Rannik, Ü., Moncrieff, J., Foken, T., Kowalski, A.S., Martin, P.H., Berbigier, P., Bernhofer, C., Clement, R., Elbers, J., Granier, A., Grünwald, T., Morgenstern, K., Pilegaard, K., Rebmann, C., Snijders, W., Valentini, R., Vesala, T., 1999. Estimates of the Annual Net Carbon and Water Exchange of Forests: The EUROFLUX Methodology. In: Fitter, A.H., Raffaelli, D.G. (Eds.), Advances in Ecological Research. Academic Press.

Baldocchi, D., 2014. Measuring fluxes of trace gases and energy between ecosystems and the atmosphere – the state and future of the eddy covariance method. Global Change Biol. 20, 3600–3609.

Bastviken, D., Thomsen, F., Svensson, T., Karlsson, S., Sandén, P., Shaw, G., Matucha, M., Oberg, G., 2007. Chloride retention in forest soil by microbial uptake and by natural chlorination of organic matter. Geochim. Cosmochim. Acta 71, 3182–3192.

Beck, H.E., Zimmermann, N.E., Mcvicar, T.R., Vergopolan, N., Berg, A., Wood, E.F., 2018. Present and future Köppen-Geiger climate classification maps at 1-km resolution. Sci. Data 5, 1–12.
Beeton, R.J.S., 1999. Advice to the Minister for the Environment, Heritage and the Arts from the Threatened Species Scientific Committee (the Committee) on Amendments to the List of Ecological Communities under the Environment Protection and Biodiversity Conservation Act 1999 (EPBC Act). In: H. A. T. A (Ed.), ADVICE TO THE MINISTER FOR THE ENVIRONMENT.
Berger, S., Braeckevelt, E., Blodau, C., Burger, M., Goebel, M., Klemm, O., Knorr, K.-H., Wagner-Riddle, C., 2019. A 1-year greenhouse gas budget of a peatland exposed to long-term nutrient infiltration and altered hydrology: high carbon uptake and methane emission. Environ. Monit. Assess. 191, 533.
Bom, 2021. Monthly rainfall, Falls Creek (Rocky Valley). VIC: BOM [Online] Available: http://www.bom.gov.au/jsp/ncc/cdio/weatherData/av?p_nccObsCode=139&p_display_type=dataFile&p_startYear=&p_c=&p_stn_num=083043 [Accessed 1/9/2019 2019].
Brubaker, K.L., Entekhabi, D., 1996. Analysis of feedback mechanisms in land-atmosphere interaction. Water Resour. Res. 32, 1343–1357.
Camac, J., Williams, R., Wahren, C.-H., Hoffmann, A., Vesk, P., 2017. Climatic warming strengthens a positive feedback between alpine shrubs and fire. Global Change Biol. 23.
Cao, S., Cao, G., Han, G., Wu, F., Lan, Y., 2020. Comparison of evapotranspiration between two alpine type wetland ecosystems in Qinghai lake basin of Qinghai Tibetan Plateau. Ecohydrol. Hydrobiol.
Cook, P.G., Herczeg, A.L., 2012. Environmental Tracers in Subsurface Hydrology. Springer Science & Business Media, Boston, MA.
Costin, A.B., 1957a. High Mountain Catchments in Victoria in Relation to Land Use. Soil Conservation Authority of Victoria, Melbourne.
De Roo, F., Zhang, S., Huq, S., Mauder, M., 2018. A semi-empirical model of the energy balance closure in the surface layer. PLOS ONE 13, e0209022.
Deb Burman, P.K., Sarma, D., Morrison, R., Karipot, A., Chakraborty, S., 2019. Seasonal variation of evapotranspiration and its effect on the surface energy budget closure at a tropical forest over north-east India. J. Earth Syst. Sci. 128, 127.
Drexler, J., Anderson, F., Snyder, R., 2008. Evapotranspiration rates and crop coefficients for a restored marsh in the Sacramento–San Joaquin Delta, California, USA. Hydrol. Processes 22, 725–735.
Duffková, R., 2013. Influence of Soil Physical Properties and Terrain Relief on Actual Evapotranspiration in the Catchment with Prevailing Arable Land Determined by Energy Balance and Bowen Ratio.
Fleischer, E., Bölter, J., Klemm, O., 2015. Summer evapotranspiration in western Siberia: a comparison between eddy covariance and Penman method formulations. Hydrol. Processes 29, 4498–4513.
Gerling, L., Weber, T.K.D., Reineke, D., Durner, W., Martin, S., Weber, S., 2019. Eddy covariance based surface-atmosphere exchange and crop coefficient determination in a mountainous peatland. Ecohydrology 12, e2047.
Göckede, M., Foken, T., Aubinet, M., Aurela, M., Banza, J., Bernhofer, C., Bonnefond, J.M., Brunet, Y., Carrara, A., Clement, R., Dellwik, E., Elbers, J., Eugster, W., Fuhrer, J., Granier, A., Grünwald, T., Heinesch, B., Janssens, I.A., Knohl, A., Koeble, R., Laurila, T., Longdoz, B., Manca, G., Marek, M., Markkanen, T., Mateus, J., Matteucci, G., Mauder, M., Migliavacca, M., Minerbi, S., Moncrieff, J., Montagnani, L., Moors, E., Ourcival, J.M., Papale, D., Pereira, J., Pilegaard, K., Pita, G., Rambal, S., Rebmann, C., Rodrigues, A., Rotenberg, E., Sanz, M.J., Sedlak, P., Seufert, G., Siebicke, L., Soussana, J.F., Valentini, R., Vesala, T., Verbeeck, H., Yakir, D., 2008. Quality control of CarboEurope flux data – Part 1: Coupling footprint analyses with flux data quality assessment to evaluate sites in forest ecosystems. Biogeosciences 5, 433–450.
Goodbrand, A., Westbrook, C.J., Van Der Kamp, G., 2019. Hydrological functions of a peatland in a Boreal Plains catchment. Hydrol. Processes 33, 562–574.
Goodrich, J.P., Campbell, D.I., Schipper, L.A., 2017. Southern Hemisphere bog persists as a strong carbon sink during droughts. Biogeosciences 14, 4563–4576.
Gorham, E., 1957. The Development of Peat Lands. Q. Rev. Biol. 32, 145–166.
Grover, S.P.P., 2001. The hydrology and characteristics of peat soils of the Victorian Alps. La Trobe University. Honours thesis.
Hamilton, S.K., 2010. Biogeochemical implications of climate change for tropical rivers and floodplains. Hydrobiologia 657, 19–35.
Hammerle, A., Haslwanter, A., Schmitt, M., Bahn, M., Tappeiner, U., Cernusca, A., Wohlfahrt, G., 2007. Eddy covariance measurements of carbon dioxide, latent and sensible energy fluxes above a meadow on a mountain slope. Boundary-Layer Meteorol. 122, 397–416.
Hirano, T., Yamada, H., Takada, M., Fujimura, Y., Fujita, H., Takahashi, H., 2016. Effects of the expansion of vascular plants in Sphagnum-dominated bog on evapotranspiration. Agric. Forest Meteorol. 220, 90–100.
Holden, J., 2005. Peatland hydrology and carbon release: why small-scale process matters. Philos. Trans. R. Soc. A: Math. Phys. Eng. Sci. 363, 2891–2913.
Horst, T.W., Weil, J.C., 1992. Footprint Estimation for Scaler Flux Mesurement in the Atmospheric Surface Layer. Boundary-Layer Meteorol. 59, 279–296.
Hou, L.G., Xiao, H.L., Si, J.H., Xiao, S.C., Zhou, M.X., Yang, Y.G., 2010. Evapotranspiration and crop coefficient of Populus euphratica Oliv forest during the growing season in the extreme arid region northwest China. Agric. Water Manage. 97, 351–356.
Howes, D.J., Fox, P., Hutton, P.H., 2015. Evapotranspiration from Natural Vegetation in the Central Valley of California: Monthly Grass Reference-Based Vegetation Coefficients and the Dual Crop Coefficient Approach. J. Hydrologic Eng. 20, 04015004.
Jegede, O.O., Foken, T., 1999. A Study of the Internal Boundary Layer due to a Roughness Change in Neutral Conditions Observed During the LINEX Field Campaigns. Theor. Appl. Climatol. 62, 31–41.
Karis, T., Silvester, E., Rees, G., 2016. Chemical regulation of alpine headwater streams during a storm event (Bogong High Plains, Victoria, Australia). J. Hydrol. 542, 317–329.
Kellner, E., 2001. Surface energy fluxes and control of evapotranspiration from a Swedish Sphagnum mire. Agric. Forest Meteorol. 110, 101–123.
Kljun, N., Calanca, P., Rotach, M.W., Schmid, H.P., 2004. A simple parameterisation for flux footprint predictions. Boundary-Layer Meteorol. 112, 503–523.
Kljun, N., Calanca, P., Rotach, M.W., Schmid, H.P., 2015. A simple two-dimensional parameterisation for Flux Footprint Prediction (FFP). Geosci. Model Dev. 8, 3695–3713.
Labadz, J., Allott, T., Evans, M., Butcher, D., Billett, M., Stainer, S., Yallop, A., Jones, P., Innerdale, M., Harmon, N., Maher, K., Bradbury, R., Mount, D., O"Brien, H., Hart, R., 2010. In: Of, I. U. P. P. S. C, Peatlands, I.O. (Eds.), Peatland Hydrology. Uk Iucn.
Lafleur, P.M., Moore, T., Roulet, N., Frolking, S., 2005. Ecosystem Respiration in a Cool Temperate Bog Depends on Peat Temperature But Not Water Table. Ecosystems 8, 619–629.
Laurance, W.F., Dell, B., Turton, S.M., Lawes, M.J., Hutley, L.B., Mccallum, H., Dale, P., Bird, M., Hardy, G., Prideaux, G., Gawne, B., Mcmahon, C.R., Yu, R., Hero, J.-M., Schwarzkopf, L., Krockenberger, A., Douglas, M., Silvester, E., Mahony, M., Vella, K., Saikia, U., Wahren, C.-H., Xu, Z., Smith, B., Cocklin, C., 2011. The 10 Australian ecosystems most vulnerable to tipping points. Biol. Conserv. 144, 1472–1480.
Lawrence, R.E., 1995. The Effects of Grazing Activity on the Hydrology of the Bogong High Plains, Australia. Rangeland J. 17, 138–153.
Leclerc, M.Y., Shen, S., Lamb, B., 1997. Observations and large-eddy simulation modeling of footprints in the lower convective boundary layer. J. Geophys. Res.: Atmos. 102, 9323–9334.
Lenters, J.D., Cutrell, G.J., Istanbulluoglu, E., Scott, D.T., Herrman, K.S., Irmak, A., Eisenhauer, D.E., 2011. Seasonal energy and water balance of a Phragmites australis-dominated wetland in the Republican River basin of south-central Nebraska (USA). J. Hydrol. 408, 19–34.
Li, M., Babel, W., Chen, X., Zhang, L., Sun, F., Wang, B., Ma, Y., Hu, Z., Foken, T., 2015. A 3-year dataset of sensible and latent heat fluxes from the Tibetan Plateau, derived using eddy covariance measurements. Theor. Appl. Climatol. 122, 457–469.
Li, Z., Yu, G.-R., Wen, X., Zhang, L.M., Ren, C.Y., Fu, Y.L., 2005. Energy balance closure ChinaFLUX sites. Sci. China Ser. D-Earth Sci. 48, 51–62.
Liljedahl, A.K., Hinzman, L.D., Harazono, Y., Zona, D., Tweedie, C.E., Hollister, R.D., Engstrom, R., Oechel, W.C., 2011. Nonlinear controls on evapotranspiration in arctic coastal wetlands. Biogeosciences 8, 3375–3389.
Liu, Y.J., Chen, J., Pan, T., 2019. Analysis of Changes in Reference Evapotranspiration, Pan Evaporation, and Actual Evapotranspiration and Their Influencing Factors in the North China Plain During 1998–2005. Earth Space Sci. 6, 1366–1377.
Lund, M., Stiegler, C., Abermann, J., Citterio, M., Hansen, B.U., Van As, D., 2017. Spatiotemporal variability in surface energy balance across tundra, snow and ice in Greenland. Ambio 46, 81–93.
Majozi, N., Mannaerts, C.M., Ramoelo, A., Mathieu, R., Nickless, A., Verhoef, W., 2016. Analysing surface energy balance closure and partitioning over a semi-arid savanna FLUXNET site in Skukuza, Kruger National Park, South Africa. Hydrol. Earth Syst. Sci. Discuss. 1–21.

Marsal, J., Marsal, J., Girona, J., Girona, J., Casadesus, J., Casadesus, J., Lopez, G., Lopez, G., Stöckle, C.O., Stöckle, C.O., 2013. Crop coefficient (K c) for apple: comparison between measurements by a weighing lysimeter and prediction by CropSyst. Irrig. Sci. 31, 455–463.
Mauder, M., Foken, T., 2004. Documentation and instruction manual of the eddy covariance software package TK2. Print, ISSN 1614-8916.
Mccartney, V.A., Silvester, E., Morgan, J.W., Suter, P.J., 2014. Physical and chemical drivers of vegetation in groundwater-source pools on the Bogong High Plains, Victoria. Aust. J. Bot. 61, 566–573.
Mitsch, W.J., Gosselink, J.G., 2007. Wetlands, Hoboken. John Wiley and Sons, New Jersey, USA, 582 pp.
Moncrieff, J., Clement, R., Finnigan, J., Meyers, T., 2004. Averaging, detrending, and filtering of eddy covariance time series. In: Lee, X., Massman, W., Law, B., A, L, Hamilton, K. (Eds.), Handbook of Micrometeorology. Springer.
Moncrieff, J.B., Massheder, J.M., De Bruin, H., Elbers, J., Friborg, T., Heusinkveld, B., Kabat, P., Scott, S., Soegaard, H., Verhoef, A., 1997. A system to measure surface fluxes of momentum, sensible heat, water vapour and carbon dioxide. J. Hydrol. 188, 589–611.
Monson, R., Baldocchi, D., 2014. Terrestrial Biosphere-Atmosphere Fluxes. Cambridge University Press, Cambridge.
Monteiro, E.B., Silva, A.C.D., Souza, A.P., Tanaka, A.A., Ferneda, B.G., Martim, C.C., 2016. Water requirements and crop coefficients of tropical forest seedlings in different shading conditions. Rev. Bras. Eng. Agríc. Ambient 20, 709–715.
Moore, P.A., Pypker, T.G., Waddington, J.M., 2013. Effect of long-term water table manipulation on peatland evapotranspiration. Agric. Forest Meteorol. 178-179, 106–119.
Ochsner, T.E., Sauer, T.J., Horton, R., 2006. Field Tests of the Soil Heat Flux Plate Method and Some Alternatives. Agronomy J. 98, 1005–1014.
Ornldaac, 2018. Fixed Sites Subsetting and Visualization Tool. ORNL DAAC, Oak Ridge. The Oak Ridge National Laboratory Distributed Active Archive Center, Tennessee, USA.
Papale, D., Reichstein, M., Aubinet, M., Canfora, E., Bernhofer, C., Kutsch, W., Longdoz, B., Rambal, S., Valentini, R., Vesala, T., Yakir, D., 2006. Towards a standardized processing of Net Ecosystem Exchange measured with eddy covariance technique: algorithms and uncertainty estimation. Biogeosciences 3, 571–583.
Pemberton, M., 2005. Australian peatlands: A brief consideration of their origin, distribution, natural values and threats. J. R. Soc. West. Australia 88, 81–89.
Pereira, L., Perrier, A., Allen, R., Alves, I., 1999. Evapotranspiration: Concepts and Future Trends. J. Irrig. Drain. Eng.-ASCE 125.
Pereira, L.S., Allen, R.G., Smith, M., Raes, D., 2015. Crop evapotranspiration estimation with FAO56: Past and future. Agric. Water Manage. 147, 4–20.
Petrone, R.M., Waddington, J.M., Price, J.S., 2001. Ecosystem scale evapotranspiration and net CO2 exchange from a restored peatland. Hydrological Process. 15, 2839–2845.
Piccinni, G., Ko, J., Marek, T., Howell, T., 2009. Determination of growth-stage-specific crop coefficients (K C) of maize and sorghum. Agric. Water Manage. 96, 1698–1704.
Pickering, C., Good, R., Green, K., 2004. Potential Effects of Global Warming on the Biota of the Australian Alps. Australian Greenhouse Office, Canberra.
Poyda, A., Reinsch, T., Skinner, R.H., Kluß, C., Loges, R., Taube, F., 2017. Comparing chamber and eddy covariance based net ecosystem CO2 exchange of fen soils. J. Plant Nutr. Soil Sci. 180, 252–266.
Rannik, Ü., Aubinet, M., Kurbanmuradov, O., Sabelfeld, K.K., Markkanen, T., Vesala, T., 2000. Footprint Analysis For Measurements Over A Heterogeneous Forest. Boundary-Layer Meteorol. 97, 137–166.
Reddy, K., Delaune, R., 2008. Biogeochemistry of Wetlands: Science and Applications, USA. CRC Press, Boca Raton, FL, USA, 2008.
Reichstein, M., Falge, E., Baldocchi, D., Papale, D., Aubinet, M., Berbigier, P., Bernhofer, C., Buchmann, N., Gilmanov, T., Granier, A., Grünwald, T., Havránková, K., Ilvesniemi, H., Janous, D., Knohl, A., Laurila, T., Lohila, A., Loustau, D., Matteucci, G., Meyers, T., Miglietta, F., Ourcival, J.M., Pumpanen, J., Rambal, S., Rotenberg, E., Sanz, M., Tenhunen, J., Seufert, G., Vaccari, F., Vesala, T., Yakir, D., Valentini, R., 2005. On the separation of net ecosystem exchange into assimilation and ecosystem respiration: review and improved algorithm. Global Change Biol. 11, 1424–1439.
Runkle, B.R.K., Wille, C., Gažović, M., Wilmking, M., Kutzbach, L., 2014. The surface energy balance and its drivers in a boreal peatland fen of northwestern Russia. J. Hydrol. 511, 359–373.
Schmid, H.P., 1997. Experimental design for flux measurements: matching scales of observations and fluxes. Agric. Forest Meteorol. 87, 179–200.
Schmid, H.P., 2002. Footprint modeling for vegetation atmosphere exchange studies: a review and perspective. Agric. Forest Meteorol. 113, 159–183.
Schmid, H.P., Lloyd, C.R., 1999. Spatial representativeness and the location bias of flux footprints over inhomogeneous areas. Adv. Ecol. Res. 93, 195.
Schuepp, P.H., Leclerc, M.Y., Macpherson, J.I., Desjardins, R.L., 1990. Footprint prediction of scalar fluxes from analytical solutions of the diffusion equation. Boundary-Layer Meteorol. 50, 355–373.
Shackleton, M., Holland, A., Stitz, L., Mcinerney, P., 2019. Macroinvertebrate Responses to Conductivity in Different Bioregions of Victoria, Australia. Environ. Toxicol. Chem. 38, 1334–1342.
Shimoyama, K., Hiyama, T., Fukushima, Y., Inoue, G., 2003. Seasonal and interannual variation in water vapor and heat fluxes in a West Siberian continental bog. J. Geophys. Res.: Atmos. 108.
Silvester, E., 2009. Ionic regulation in an alpine peatland in the Bogong High Plains, Victoria, Australia. Environ. Chem. 6.
Silvester, E., Karis, T., Yusuf, A., Pengelly, J., Grover, S., Rees, G.N., 2021. Organic carbon and nitrogen dynamics during a peatland storm event: How dissolved combined amino acids reveal the spatial and temporal separation of organic molecules. J. Hydrol. 597, 126191.
Stannard, D.I., Gannett, M.W., Polette, D.J., Cameron, J.M., Waibel, M.S., Spears, J.M., 2013. Evapotranspiration from marsh and open-water sites at Upper Klamath Lake, Oregon, 2008–2010. Scientific Investigations Report, Reston, VA.
Swindles, G.T., Morris, P.J., Mullan, D.J., Payne, R.J., Roland, T.P., Amesbury, M.J., Lamentowicz, M., Turner, T.E., Gallego-Sala, A., Sim, T., Barr, I.D., Blaauw, M., Blundell, A., Chambers, F.M., Charman, D.J., Feurdean, A., Galloway, J.M., Gałka, M., Green, S.M., Kajukało, K., Karofeld, E., Korhola, A., Lamentowicz, Ł., Langdon, P., Marcisz, K., Mauquoy, D., Mazei, Y.A., Mckeown, M.M., Mitchell, E.A.D., Novenko, E., Plunkett, G., Roe, H.M., Schoning, K., Sillasoo, Ü., Tsyganov, A.N., Van Der Linden, M., Väliranta, M., Warner, B., 2019. Widespread drying of European peatlands in recent centuries. Nat. Geosci.
Tanner, C.B., Fuchs, M., 1968. Evaporation from unsaturated surfaces: A generalized combination method. J. Geophys. Res. 73, 1299–1304, 1896-1977.
Vickers, D., Mahrt, L., 1997. Quality Control and Flux Sampling Problems for Tower and Aircraft Data. J. Atmos. Oceanic Technol. 14, 512–526.
Wang, K., Dickinson, R.E., 2012. A review of global terrestrial evapotranspiration: Observation, modeling, climatology, and climatic variability. Rev. Geophys. 50.
Webb, E.K., Pearman, G.I., Leuning, R., 1980. Correction of flux measurements for density effects due to heat and water vapour transfer. Q. J. R. Meteorol. Soc. 106, 85–100.
Weiss, R., Shurpali, N., Sallantaus, T., Laiho, R., Laine, J., Alm, J., 2006. Simulation of water table level and peat temperatures in boreal peatlands. Ecol. Modell. 192, 441–456.
Western, A., Siriwardena, L., Lawrence, R., Rutherfurd, I., 2008. In: Sponges or Wicks?: What Is the Role of Bogs in Hydrological Response on the Bogong High Plains? Proceedings of Water Down Under 2008. Adelaide.
Whinam, J., Chilcott, N., Morgan, J., 2003. Floristic composition and environmental relationships of Sphagnum dominated communities in Victoria. Cunninghamia 8 (2), 2003.
Wilczak, J., Oncley, S., Stage, S., 2001. Sonic Anemometer Tilt Correction Algorithms. Boundary-Layer Meteorol. 99, 127–150.
Williams, R.J., 1987. Patterns of air temperature and accumulation of snow in subalpine heathlands and grasslands on the Bogong High Plains, Victoria. Aust. J. Ecol. 12, 153–163.
Wilson, K.B., Baldocchi, D.D., 2000. Seasonal and interannual variability of energy fluxes over a broadleaved temperate deciduous forest in North America. Agric. Forest Meteorol. 100, 1–18.
Worboys, G.L., Good, R.B., 2011. Caring For Our Australian Alps Catchments: Summary Report For Policy Makers. Department of Climate Change and Energy Efficiency, Canberra.
Wu, J., Kutzbach, L., Jager, D., Wille, C., Wilmking, M., 2010. Evapotranspiration dynamics in a boreal peatland and its impact on the water and energy balance. J. Geophys. Res.: Biogeosci. 115.
Xu, J., Morris, P.J., Liu, J., Holden, J., 2018a. PEATMAP: Refining estimates of global peatland distribution based on a meta-analysis. CATENA 160, 134–140.

Xu, K., Metzger, S., Desai, A.R., 2018b. Surface-atmosphere exchange in a box: Space-time resolved storage and net vertical fluxes from tower-based eddy covariance. Agric. Forest Meteorol. 255 (81-91), 255, 81-91.

Xueqin, Z., Yu, R., Zhi-Yong, Y., Zhenyao, L., Du, Z., 2009. Spatial and temporal variation patterns of reference evapotranspiration across the Qinghai-Tibetan Plateau during 1971–2004. J. Geophys. Res. - Atmos. 114, D15105.

Zhao, P., Kang, S., Li, S., Ding, R., Tong, L., Du, T., 2018. Seasonal variations in vineyard ET partitioning and dual crop coefficients correlate with canopy development and surface soil moisture. Agric. Water Manage. 197, 19–33.

Zhou, L., Zhou, G., 2009. Measurement and modeling of evapotranspiration over a reed (Phragmites australis) marsh in Northeast China. J. Hydrol. 372, 41–47.